Purdue University
Purdue e-Pubs

International High Performance Buildings Conference

School of Mechanical Engineering

2014

Solar Optical Properties of Roller Shades: Modeling Approaches, Measured Results and Impact on Energy Use and Visual Comfort

Ying-Chieh Chan
School of Civil Engineering, Purdue University, 550 Stadium Mall Dr., West Lafayette, IN 47907 USA / Ray W. Herrick Laboratories, School of Mechanical Engineering, Purdue University, 140 S. Martin Jischke Dr., West Lafayette, IN 47907, USA, ychan@purdue.edu

Athanasios Tzempelikos
ttzempel@purdue.edu

Brent Protzman
Lutron Electronics Co. Inc., 7200 Suter Rd., Coopersburg, PA 18036 USA, bprotzman@lutron.com

Solar Optical Properties of Roller Shades: Modeling Approaches, Measured Results and Impact on Daylighting and Visual Comfort

Ying-Chieh CHAN[1,2*], Athanasios TZEMPELIKOS[1,2], Brent PROTZMAN[3]

[1]*School of Civil Engineering, Purdue University*
550 Stadium Mall Dr., West Lafayette, IN 47907 USA

[2]*Ray W. Herrick Laboratories, School of Mechanical Engineering, Purdue University*
140 S. Martin Jischke Dr., West Lafayette, IN 47907, USA

[3]*Lutron Electronics Co. Inc.,*
7200 Suter Rd., Coopersburg, PA 18036 USA

* Corresponding Author

ABSTRACT

One of the challenges with dynamic facades is how to balance the need for daylight versus reducing overall energy use while ensuring comfort for the occupants. This requires detailed knowledge of the solar optical properties of fenestration, which affect the transmission of solar gains and daylight. Although there is adequate information, databases and tools for spectral and angular glazing properties, there is less available information on shading systems. Complex fenestration systems, such as venetian blinds, have been studied and characterized using advanced experimental and computational methods such as bi-directional distribution functions. Nevertheless, there are very limited studies on the solar-optical properties of roller shades, which are very common in commercial buildings. In most existing studies and simulation tools, the properties of roller shades are assumed constant and diffuse. The only available semi-empirical model showed that roller shade properties may have strong direct components and angular variation, depending on the openness factor and fabric color (equivalently, direct and diffuse transmittance). These can affect the energy and daylighting performance, as well as their impact on glare.
This paper first provides an overview of current approaches for modeling solar optical properties of roller shades, including advantages and limitations. Then, integrating sphere measurements were conducted to determine the detailed solar optical properties of different products. The results are compared to previous findings and provide useful information about direct-direct, direct-diffuse and angular properties of roller shades, depending on openness factor and color. Finally, the impact of detailed solar optical properties on daylight performance and glare is evaluated using annual simulation results for different fabrics. The results show that detailed shading properties should be used for a more realistic evaluation of the impact of shading on daylighting and visual comfort.

1. INTRODUCTION

High performance commercial facades rely on fenestration systems to control glare and solar heat gains. Recent efforts have concentrated on developing efficient dynamic shading controls, and links with lighting and HVAC controls. One of the challenges is how to balance the need for daylight versus reducing overall energy use while ensuring comfort for the occupants seated near the facade. Studies have shown that roller shades have potential to reduce energy consumptions associated with fenestration system through proper design and control (Wankanapon and Mistrick 2011; Shen and Tzempelikos 2012; Tzempelikos and Shen 2013). Knowledge of detailed solar optical properties of fenestration, which affect the transmission of solar gains and daylight, will also affect the accuracy of energy modeling and glare evaluation.

For most of the existing thermal and daylighting calculation tools and modules, the detailed energy consumption and daylight metrics associated with fenestration systems can only be obtained if the solar optical and the thermal properties of individual layers of a glazing/shading system are known. The solar optical properties vary with incident angle. For glazing systems, the angular-based solar optical properties are available from the International Glazing Database (IGDB 2014) and can be exported through LBNL's WINDOW software (LBNL 2011). LBNL also published a Complex Glazing Database (CGDB 2014) which attempts to collect measured solar optical properties as well as associated and measured BSDF (bidirectional scattering distribution function) files for different complex fenestration systems such as woven shades, venetian blinds, etc.

BSDF is an approach to describe angle-dependent solar optical properties considering both the incident and outgoing directions (Andersen and de Boer 2006). This information can be collected through advanced experimental techniques such as a goniophotometer (Andersen et al. 2010) or a spectrophotometer (Nilsson and Jonsson 2010). However, such instruments and procedures are quite expensive and time-consuming. Nevertheless, the size of the current database is not sufficient for design simulation since there are hundreds or thousands of products available. Instead of measurements, ray tracing simulation can also be applied to generate BSDF functions (McNeil et al. 2013). The challenge of using this method for roller shades (especially woven type) is the complexity of the microstructure of the fabric. The BSDF function generated from WINDOW software or *genBSDF* of Radiance can be directly used in EnergyPlus and Radiance simulation.

Roller shades come in a wide variety of colors and patterns with varying degrees of shading and weave constructions that result in different degrees of openness and transmission characteristics. The term "openness factor" described by manufactures usually refers to the "open" or "see-through" percentage of the shade (fabric). When direct radiation strikes the shade surface, it is split into two portions: the unobstructed portion which is transmitted directly through the openings (beam-beam portion), and the interrupted portion—some of which will be scattered in the forward direction (transmitted), scattered in the reverse direction (reflected), or be absorbed. Therefore, except for the angular dependence, we also need to consider a beam/diffuse split of solar radiation or illuminance through roller shades (this process is not necessary for common glazing products).

Usually, fabric manufactures only provide a single value of total transmittance and reflectance at normal incidence when demonstrating or specifying their products. Therefore, an approach to estimate the off-normal and diffuse properties from such limited information is desired and is important for more accurate thermal and daylighting modeling. Very few existing models consider the angular-based solar properties of roller shades. is the only complete semi-empirical model (Kotey et al. 2009) predicts the angular-dependent transmittance by only using measured beam-beam and beam-total transmittance at normal incidence.

This paper reviews the most-widely used assumptions and methods of modeling the solar optical properties of roller shades. Detailed measured properties of different fabrics are used to evaluate differences between existing approaches and provide useful information about direct-direct, direct-diffuse and angular properties of roller shades, depending on openness factor and color. Finally, the impact of different evaluation methods on energy use, daylight performance and glare is discussed using annual simulation results for different fabrics, orientations and climates.

2. EXISTING MODELS FOR ROLLER SHADE SOLAR OPTICAL PROPERTIES

This section presents the existing assumptions and models used to predict the solar optical properties of roller shades when information is limited (e.g., these models do not require inputs of angular or direct-diffuse properties). **Table 1** summarizes the methods and required input data. Detailed descriptions are presented in the following sections.

2.1 Simplified Non-Angular Properties Model

The widely used energy simulation software, EnergyPlus (2007), only allows the user to input one value of solar and visible transmittance (and reflectance) to model roller shades (except using advanced BSDF functions generated from the CGDB database). Normally, the transmittance and reflectance at normal incidence are used. The model assumes that the fabric materials are perfectly diffusing and have no angular differences and the model treats both direct illuminance and diffuse illuminance using the same transmittance value (beam-total transmittance equals to diffuse-diffuse transmittance). This assumption is unable to accurately represent shade performance in most of the cases, especially for fabrics with noticeable openness.

Radiance's translucent function (*trans function*) further allows the users to define beam/diffuse ratio, thus improving accuracy, but still does not consider angular differences. However, Apian-Bennewitz (2013) pointed out that this function is the most suitable one for Radiance (for modeling roller shades) when BSDF information or other angular solar optical properties are not available.

Reinhart and Andersen (2006) validated the accuracy of *trans function* when applied in cases with translucent glass. The measured indoor illuminance results showed that using direct normal transmittance as an input in *trans function* will result in overestimation because *trans function* is not angular dependent. When using direct normal transmittance as the input, the ray-tracing algorithm applies the same transmittance value to the entire calculation even including diffuse-diffuse portion. They suggested that using (measured) diffuse-diffuse transmittance to replace direct-total transmittance at normal incidence; and following this approach, the indoor illuminance distribution showed a good agreement when compared to measured results under both cloudy and sunny conditions. Nevertheless, one should note that this case study does not validate the accuracy when there is a beam-to-beam component because their validation target is translucent glass and it is assumed to have perfectly diffuse properties. In addition, manufacturers usually do not provide diffuse-diffuse transmittance of shading product. In their study, they used angular measured results to calculated diffuse-diffuse transmittance.

Apian-Bennewitz (2013) compared the simulation results of Radiance modeled using BSDF function and *trans* function and found that properties of angular dependent materials (including most roller shade fabrics) are not well matched by *trans function*, because their transmission parameters depend on the incident direction but there are still some pros such as the low number of input parameters. Deneyer (2014) compared the workplane illuminance modeled by a measured BSDF function to the results modeled by a Lambertian function (perfect diffuse function) and observed that BSDF function has an important impact on workplane illuminance close to the window.

Table 1: Summary of available Models to obtain Solar Optical Properties of roller shades

Model	Reference	Required Input Data
Simplified non-angular properties model	Radiance – trans function (Reinhart and Andersen 2006)	Beam-total transmittance at normal incidence or Diffuse-diffuse transmittance Beam/diffuse ratio (specular transmitted value)
	EnergyPlus (2007)	Beam-total transmittance at normal incidence
Semi- Empirical Model	Kotey et al. (2009)	Beam-total transmittance at normal incidence Beam-beam transmittance at normal incidence
Ray Tracing Model	Radiance – *genBSDF* (McNeil et al. 2013)	Detailed geometry of the fabric
Geometrical Radiosity Model	Window Software (Carli Inc. 2006)	Geometry of the fabric (spacing and thread thickness)

2.2 Kotey et al. Semi-Empirical Model (Kotey et al. 2009)

Kotey et al. (2009) developed a semi-empirical model for direct-direct, direct-diffuse and angular shade properties from detailed integrated sphere measurements (Collins et al. 2012) of the spectral beam-beam transmittance, beam-diffuse transmittance, and beam-diffuse reflectance at incident angles ranging from 0° to 60°. They first converted the spectral data to solar optical properties (ex: solar and visible transmittance/reflectance) according to ASTM standards and fitted a cosine power function to the measured properties at different incident angles. The reason for cosine correlation was the symmetrical and adjustable shape of the function. The details of the semi-empirical model are described below.

Beam-beam Transmittance

The normalized beam-beam shade transmittance $norm_{\tau bb}$ is calculated from:

$$norm_{\tau_{bb}} = \frac{\tau_{bb}(\theta)}{\tau_{bb}\left(\theta = 0\right)} = \cos^{b}\left(\frac{\theta}{\theta_{cutoff}}\frac{\pi}{2}\right) \qquad \theta \le \theta_{cutoff} \tag{1}$$

$$b = 0.6\cos^{0.3}\left(\tau_{bb}\left(\theta = 0\right)\frac{\pi}{2}\right) \tag{2}$$

$$\theta_{cutoff} = 65° + (95° - 65°)(1 - \cos(\tau_{bb}\left(\theta = 0\right)\frac{\pi}{2})) \tag{3}$$

where $\tau_{bb}(\theta)$ is beam-beam transmittance at incident angle θ. A cut-off angle θ_{cutoff} is used to denote that the transmittance reduces to zero beyond a certain angle. The fabric openness factor is assumed to be equal to τ_{bb} when the incidence angle is zero.

Beam-total Transmittance
The normalized beam-beam shade transmittance $norm_{\tau bt}$ is calculated from:

$$norm_{\tau_{bt}} = \frac{\tau_{bt}(\theta)}{\tau_{bt}\left(\theta = 0\right)} = \cos^{d}(\theta) \qquad \theta \le \theta_{cutoff} \tag{4}$$

$$\tau^{str} = \frac{\tau_{bt}(\theta = 0) - \tau_{bb}(\theta = 0)}{1 - \tau_{bb}(\theta = 0)} \tag{5}$$

$$\begin{aligned} d &= 0.133(\tau^{str} + 0.003)^{-0.467} && 0 \le \tau^{str} \le 0.33 \\ d &= 0.33(1 - \tau^{str}) && 0.33 \le \tau^{str} \le 1 \end{aligned} \tag{6}$$

where $\tau_{bt}(\theta)$ is beam-total transmittance at incident angle θ. Most of the manufacturers provide beam-total transmittance at normal incidence (single value for solar and/or visible spectrum). The cut-off angle for beam-total transmittance is not as straightforward as beam-beam transmittance. Here, the cut-off angle restriction is only applied for the dark-color samples due to limited scattered reflection or transmission. However, the criteria for separating classify light-color and dark-color fabrics are not clear.

Beam-diffuse transmittance
The beam-diffuse transmittance is calculated from the beam-total minus the beam-beam respective values for every angle. This property is important when calculating illuminance distributions and affects glare performance.

Diffuse-diffuse Transmittance
The diffuse-diffuse transmittance is calculated from integration of direct-total transmittance over the hemisphere (cannot be measured directly):

$$\tau_{dd} = 2\int_{0}^{\pi/2} \tau_{bt}(\theta)\cos(\theta)\sin(\theta)d\theta \tag{7}$$

2.3 BSDF Ray Tracing Model

genBSDF is an open source Radiance tool which creates two hemispheres (one for transmission and one for reflection) to receive emitted rays (McNeil et al. 2013). The origins of emitted rays are randomly distributed over the emitting surface and ray directions are randomly distributed within the range of angles defined by the angular boundaries of the Klems patch. Combined with Radiance's *rtcontrib* function, *genBSDF* is able to record and track each ray's exiting direction. McNeil et al. (2013) showed that the simulated transmittance results of a micro-perforated shading system are very close to the results measured by a goniophotometer. They concluded that the BSDFs generated via *genBSDF* are reasonably accurate. However, the microstructure of micro-perforated shading system is relatively simple when compared to open-weave roller shade fabrics.

2.4 LBNL Geometrical Radiosity Model

WINDOW software has incorporated a woven shade screen model that uses the geometrical radiosity method to estimate BSDFs of woven shades. The model assumes that the threads are Lambertian and opaque and the geometry is a square pattern with constant spacing and thread thickness (Carli Inc. 2006). Jonsson et al. (2008) compared the results calculated by this model with experimental data and the agreement was not good. The source of error was not identified, but future versions of WINDOW will have corrections.

3. DETAILED MEASUREMENTS OF SHADE PROPERTIES FOR VALIDATING AND COMPARING RESULTS

An integrating sphere originally designed to measure solar optical properties at normal incidence was redesigned by Collins et al. (2012) to measure the off-normal optical properties described by Kotey et al. (2009). The integrating sphere can separate the unobstructed and the scattered components of incident beam radiation. However, this measurement method can only be used to obtain beam-beam and beam-total transmittance and reflectance and cannot be used to measure detailed scattering function (i.e., BSDF functions). The uncertainty of this method is ±3%.

In this study, six different shade fabrics were tested to obtain their properties at normal incidence, and two of these fabrics were measured using the method described above to obtain the angular beam-beam and beam-total transmittance values. **Table 2** summarizes the measured results and the data provided by the manufacturers. Theoretically, the beam-to-beam transmittance at normal incidence should be close to the openness factor, so the openness factor provided by manufacturer was compared to the measured beam-beam transmittance at normal incidence. The measurements cover different colors, openness factors, and total transmittance values. When the openness factor or τ_{bb} is close to τ_{bt}, it means that there is little direct-diffuse transmission and most of the light transmitted is still direct.

The relative error seems high when the openness factor is small (Fabrics 1-2), but it will not cause noticeable errors when further calculating daylight metrics. Fabric 4 is an oyster (light color) fabric with 5% openness and 14 % listed total transmittance –there is a strong direct-diffuse component; for this case, the measurements showed that the actual beam-total transmittance is 24.2%, introducing unacceptable errors for both beam-total transmittance (72.8%) and beam-beam transmittance (38%). Such results indicate that data provided by manufactures is not always accurate. The listed properties of Fabric 6, which also has a significant direct-diffuse component, are in better agreement with measured data.

Table 2: Measured Transmittance at Normal Incidence and Data Provided by Manufacturers

Fabric #	1	2	3	4	5	6
Fabric Color	Charcoal	White /Linen	Steel Grey /Silver	Oyster	Charcoal	Linen
τ_{bt} (Manufacturer)	1%	10%	5%	14%	11%	23%
τ_{bt} (Measured)	1.30%	10.50%	5%	24.20%	10.90%	22.20%
Error	**30.00%**	**5.00%**	**0.00%**	**72.86%**	**-0.91%**	**-3.48%**
Openness Factor	1%	1%	4%	5%	10%	10%
τ_{bb} (Measured)	1.30%	1.60%	4.20%	6.90%	9.70%	11.20%
Error	**30.00%**	**60.00%**	**5.00%**	**38.00%**	**-3.00%**	**12.00%**

4. COMPARISON OF SEMI-EMPIRICAL MODEL WITH MEASUREMENTS OF ANGULAR SOLAR OPTICAL PROPERTIES

The results of the semi-empirical model developed by Kotey et al. (2009) were compared to detailed integrated sphere measurements for angular properties of two different fabrics (Fabrics 3 and 4 in Table 2). The required inputs τ_{bt} (θ=0) and τ_{bb} (θ=0) in the semi-empirical are taken from measured results, and the criteria to categorize shade color is front reflectance of the fabric. When front reflectance greater than 0.5, the fabric would be classified as light-color fabric; otherwise, it would be classified as dark-color fabric.

Fabric 3

Fabric 3 is a high performance shade with different colors on the front and back side. The color of the exterior side is reflective silver (ρ=77%) for reflecting solar radiation to the outside and prevent over-heating issues. The interior side has a steel grey color. The shade has a 4% openness and 5% normal τ_{bt} so there is a strong direct component.

Figure 1 shows the comparison between measurements and the empirical model for both beam-beam and beam-total transmittance. The differences are less than 1%. However, the measurements showed that τ_{bt} is almost constant for incidence angles smaller than 30°, which was be captured by the empirical model (since a cosine function is used). Overall, the semi-empirical model slightly underestimates τ_{bt} and slightly overestimates τ_{bb} for this fabric type –the impact of these differences on daylight levels and glare is presented in the next section. Note that τ_{bt} is also not zero beyond 60° incidence angle. Finally, the diffuse-diffuse transmittance for this fabric is equal to 3.67% according to measurements and 3.25% according to the model.

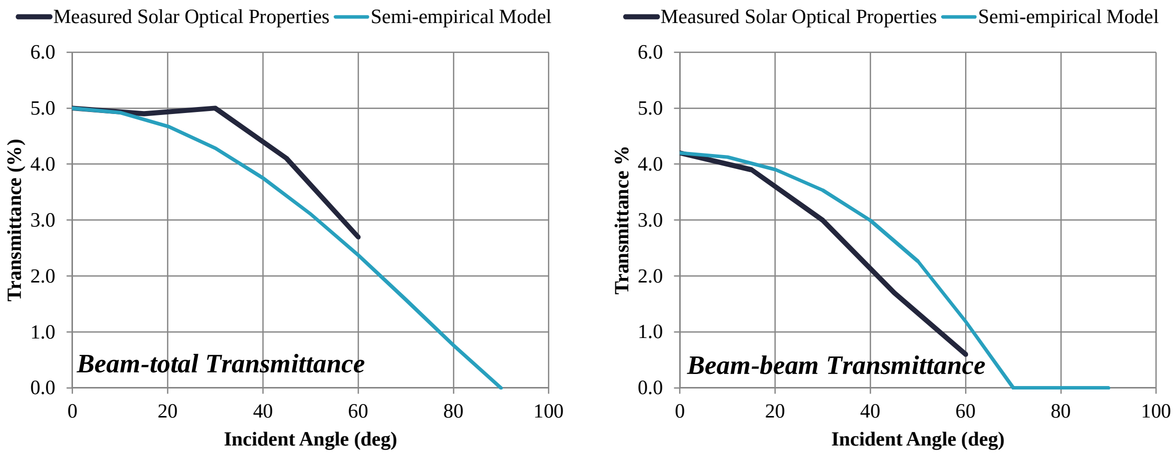

Figure 1: Comparison between angular Beam-total and Beam-beam Transmittance (measurements vs semi-empirical model) for Fabric 3

Fabric 4

Fabric 4 is a commonly used light-colored product with 5% openness and $\tau_{bt}(\theta=0)$ is 24%, therefore, direct-diffuse transmission is dominant (note that this is the fabric with the largest error in manufacturer's data). The beam-total transmittance results of the semi-empirical model showed a very good agreement with measured data (Figure 2), while τ_{bb} is again slightly overestimated. This fabric has a significant value of transmittance beyond 60° that cannot be neglected. The diffuse-diffuse transmittance for this fabric is equal to 19.75% according to measurements and 21.14% according to the model.

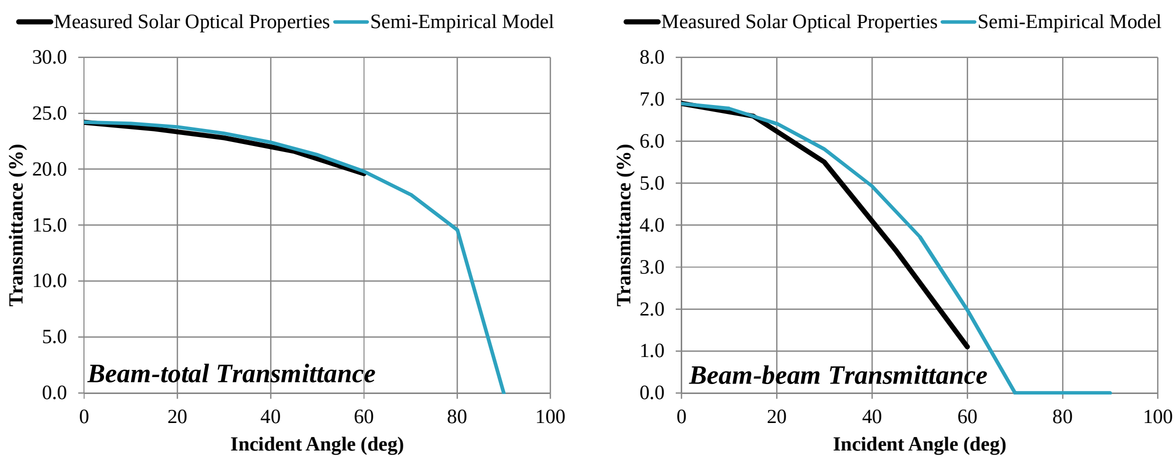

Figure 2: Comparison between angular Beam-total and Beam-beam Transmittance (measurements vs semi-empirical model) for Fabric 4

5. IMPACT OF DIFFERENT MODELING APPROACHES ON INDOOR ILLUMINANCE LEVELS AND DAYLIGHT GLARE EVALUATION

The differences in predicted shading properties (angular and direct-diffuse components) according to the different approaches have an impact on daylight levels, glare evaluation and solar gains estimation, when used in building simulation for static or dynamic (annual) analysis. This section discusses these impacts and elaborates on the differences between the different methods.

To compare between the different models, a hybrid ray tracing and radiosity method (Chan and Tzempelikos 2012) is used to simulate indoor illuminance and daylight glare probability. The accuracy of this method has been validated with full-scale experiments and with Radiance. There are four major parts in simulation process: 1) predicting the amount of direct, sky diffuse, and ground diffuse illuminance on the windows, 2) predicting the amount of direct and diffuse light transmitted through (complex) fenestration, including controls if needed, 3) simulating interior inter-reflections to obtain interior illuminance distributions and daylight metrics, and 4) simulating glare from daylight using appropriate indices. The solar optical properties modeling is embedded in the second step.

For glare evaluation, the daylight glare probability (DGP) is used as an indicator (Wienold and Christoffersen 2006), since it is the latest daylight glare index generally accepted and presented a good fit with occupant survey results related to visual comfort.

5.1. Comparison of Different Modeling Approaches with Full-Scale Experiments – Work Plane Illuminance

First, a comparison between modeled results and full-scale experiments is performed, in order to estimate the range of differences between models as well as to further validate the hybrid method against measured data in real spaces equipped with roller shades. The experiments were conducted in the facade engineering laboratories of Purdue University in West Lafayette, Indiana. This research facility was specifically designed for quantifying the impact of façade design options and related controls on indoor environmental conditions and energy use. Two identical, side-by-side test office spaces with reconfigurable facades (**Figure 3**) were used to compare the performance of different glazing and shading options under real weather conditions for several months. The dimensions of each room are 5m wide by 5.2m deep by 3.4m high, with a glass façade (60% window-to-wall ratio) facing south. A detailed description of the experimental setup and instrumentation can be found in Shen et al. (2013).

For the results presented in this paper, the façade was equipped with a high performance glazing unit (Solaban70XL-clear), that has a selective low-e coating (τ_v=65% at normal incidence). Fabric 3 of Table 2 was installed in both spaces. The shades were closed (since the purpose of this work was to compare between different modeling approaches with respect to shading properties), but shading devices can be controlled automatically (through customized software) or manually, and are connected to the lighting control system and to the data acquisition and monitoring system. Several photometers are used to measure light levels, both exterior (horizontal and vertical illuminance) and interior (transmitted through window, horizontal work plane illuminance at 6 points in each room, and at variable positions at the observer's eye height level for vertical illuminance measurements). A vertical exterior solar pyranometer provides information about the direct and diffuse portions of solar radiation and illuminance. All sensors are connected to a data acquisition and control system, controllable through remote access in order to run experiments without interfering with human presence. Illuminance levels were recorded every minute, for different measurement periods from October 2013-April 2014.

The spaces were modeled using the hybrid radiosity and ray-tracing method, with the shading properties were modeled using the approaches described in Section 2. In this way, work plane illuminance distributions are compared between each method and experimental measurements. In particular, two ways of using constant properties for roller shades were considered: (i) constant τ_{bt} with no specular components (τ_{dd} = τ_{bt} at normal incidence) and (ii) constant τ_{bt} and τ_{bb} with a fixed beam-diffuse ratio without angular dependence. The measured values of τ_{bb} and τ_{bt} (Table 2) were used as inputs to these models to increase accuracy. Except for these, the comparison also includes properties obtained using the detailed integrated sphere measurements, by the semi-empirical model, as well as illuminance values from the full-scale experimental measurements.

Figure 4 presents sample work plane illuminance results for two successive days in October 2013 (desk located 1.6m away from the windows). The first day is sunny and the second day is mix condition, with cloud cover during the afternoon. The semi-empirical model and the detailed measured properties showed good agreement with experimental data. Small differences are due to uncertainties of modeled values and assumptions in the hybrid method, however these differences are within the desired prediction error and the model has been previously validated (Chan and Tzempelikos, 2012). The two methods with constant properties both fail to predict illuminance values correctly. The model with no specular transmission cannot detect beam-beam components, therefore it significantly underestimates work plane illuminance (when no direct sunlight is present, it overestimates illuminance as described next). The model with constant fixed beam-diffuse ratio overestimates work plane illuminance since it does not consider the angular variation of transmittance.

Figure 3: Exterior and interior view of test offices used for experimental measurements

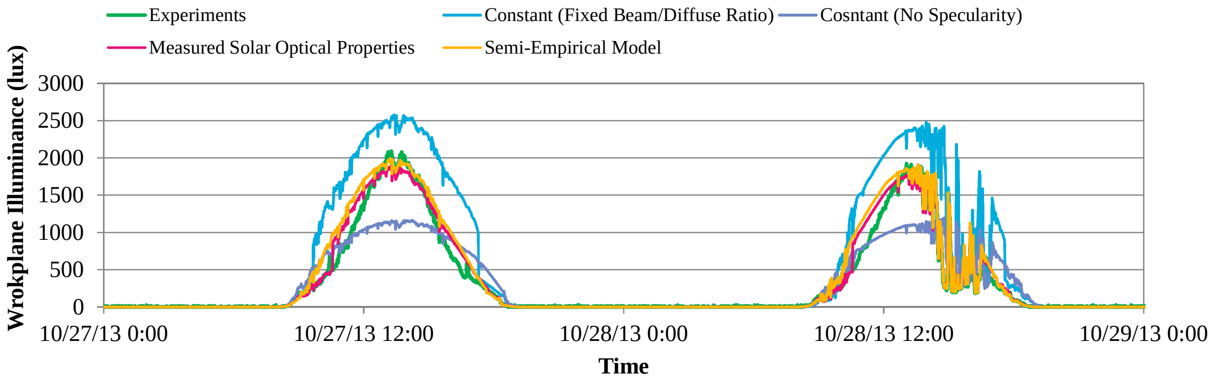

Figure 4: Comparison of Workplane Illuminance values between different properties modeling methods and experimental measurements.

5.2. Comparison between Modeling Methods Using Annual Daylighting Simulation

To estimate the overall impact of property modeling methods on daylight distributions and daylight metrics, a case study was performed with annual daylighting calculations, for a typical perimeter office space (5m by 5m by 3m high) located in Chicago. A double-clear glazing unit (normal visible transmittance =78.6%) was used in this case. Fabrics 3 and 4 of Table 2 (for which we have detailed measured properties) were modeled as fully closed. Detailed illuminance distributions, vertical illuminance at the eye level and DGP were calculated for the entire year for every case. Representative results of work plane illuminance for summer and winter days are shown in Figures 5-8 and annual metrics are presented in Table 3.

5.2.1 Work plane illuminance - Fabric 3

Figure 5 and Figure 6 show work plane illuminance results with Fabric 3 at 2.5m from the window in winter and summer respectively. The first and third days in winter are sunny; in summer, the first three days are sunny. In winter, the fabric beam-beam component allows some direct light to reach the work plane –this is similar to the validation case presented above. The semi-empirical model and the detailed properties model result in almost identical values. The constant model with no specularity both overestimates and underestimates values depending on sky conditions, but the differences are within an acceptable range.

In the summer, there is no direct sunlight on the work plane, therefore beam-diffuse properties are significant and the constant model with no specularity fails to predict illuminance values (significantly overestimates results in this case). The constant model with fixed beam/diffuse ratio highly overestimates work plane illuminance in winter and summer since no angular variation is considered.

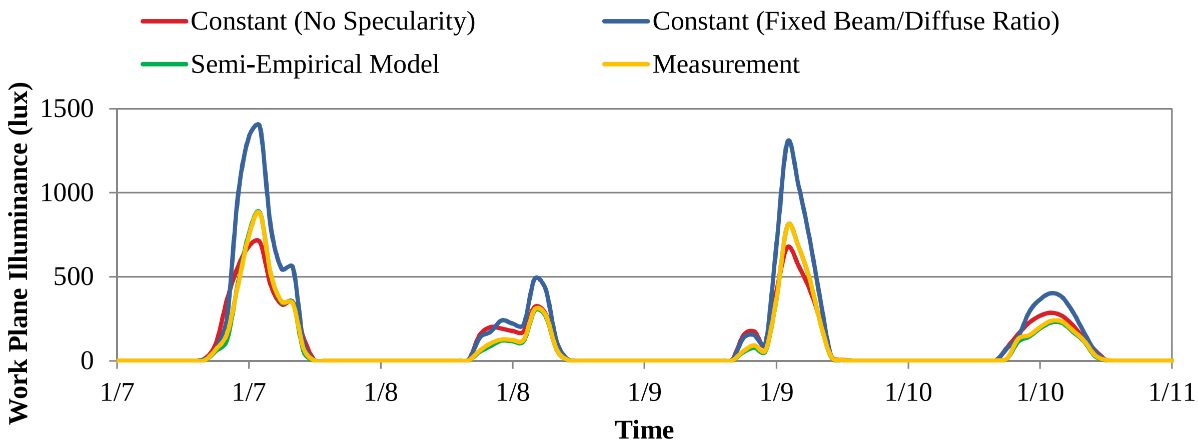

Figure 5: Comparison of Workplane Illuminance in Winter for Fabric 3

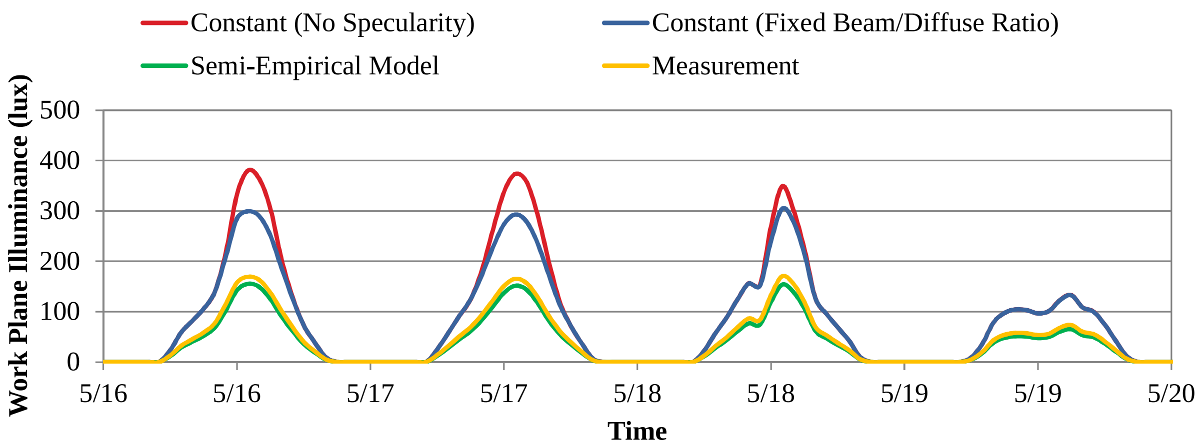

Figure 6: Comparison of Workplane Illuminance in Summer for Fabric 3

5.2.2 Work plane illuminance - Fabric 4
Similar results are shown in Figure 7 and Figure 8 for Fabric 4 (lighter color, higher beam-diffuse ratio so the values are higher in this case). During overcast days, the effect of beam-diffuse transmission is significant. The results obtained from constant properties result in significant errors, especially in the summer.

5.2.3 Annual glare evaluation and overall comparison
Annual distributions of DGP were also computed for the two fabrics. Data was collected for every hour in the year, according to the luminance in the field of view, window luminances and position index according to the original DGP equation. Figure 9 shows the annual DGP distribution (in the form of temporal graphs) for Fabric 3. Since the transmittance of this fabric is low and the shades are closed, there is no noticeable glare for any of the cases.

Nevertheless, the DGP index in the case with constant properties and no specular transmittance is higher than the rest.

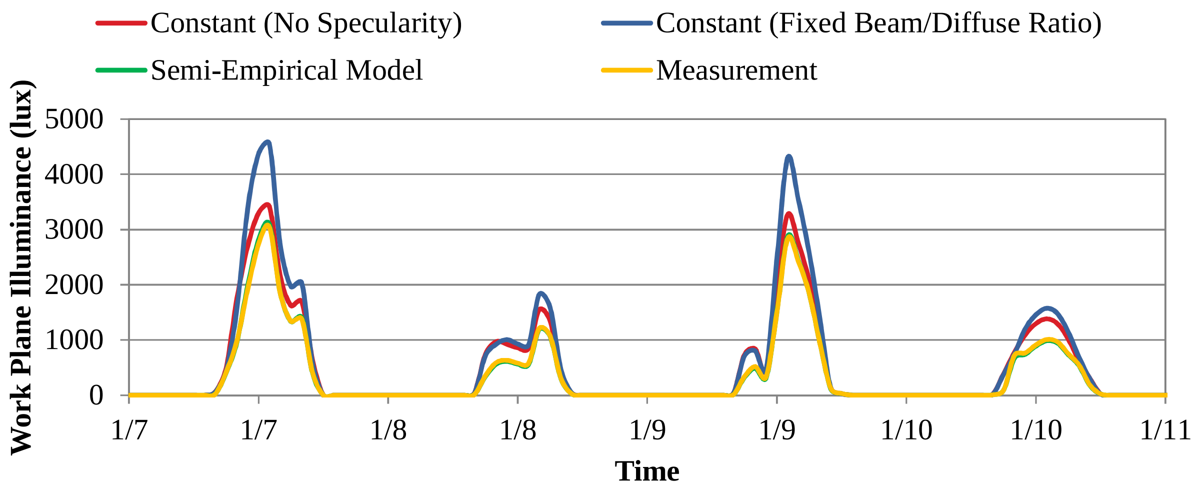

Figure 7: Comparison of Workplane Illuminance in Winter for Fabric 4

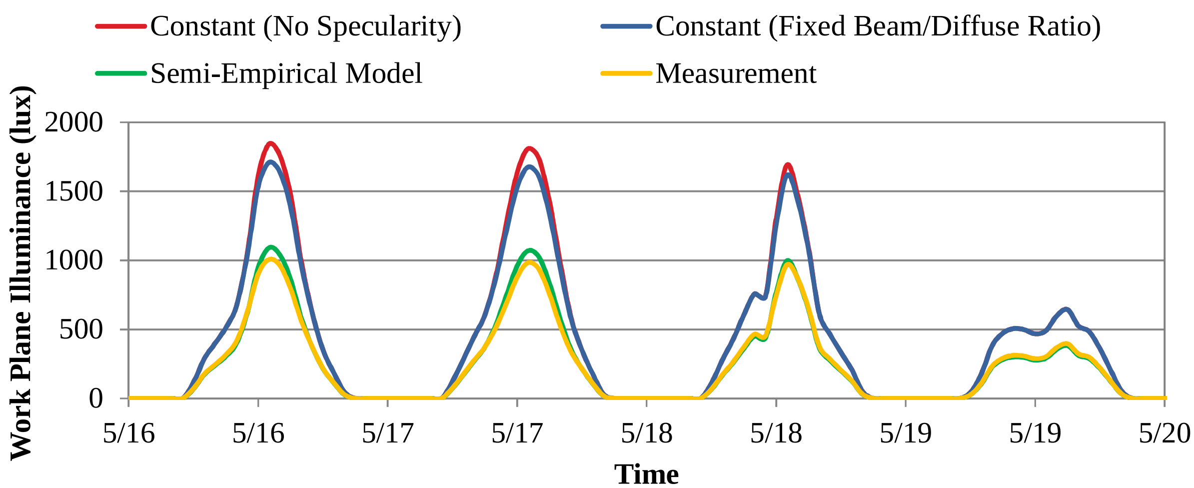

Figure 8: Comparison of Workplane Illuminance in Summer for Fabric 4

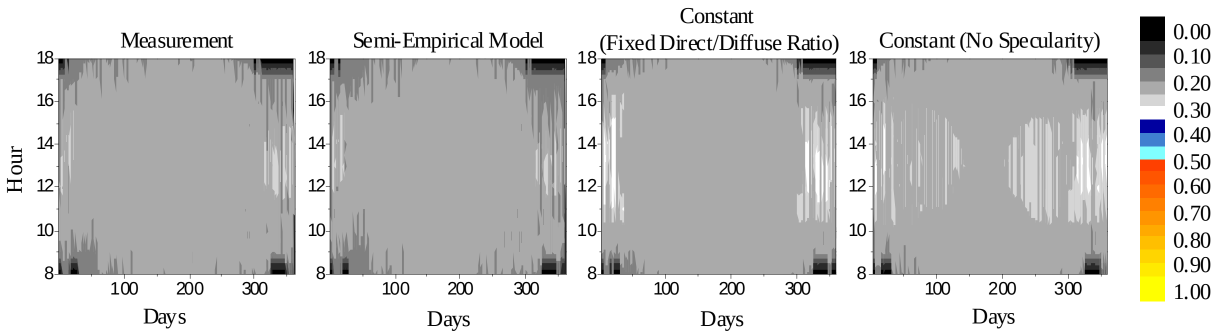

Figure 9: Annual DGP distribution with Fabric 3

DGP annual distributions for Fabric 4 are shown in Figure 10. The higher transmittance and significant direct-diffuse component of this fabric result in several glare hours in the year. Although the work illuminance calculated from the measured properties and the semi-empirical model were very close, the distribution of DGP is a bit different due to differences in the luminance field and vertical illuminance at the eye. Note that the constant properties models overestimate glare for the entire year. The distribution of constant no specularity model is very different to all the others.

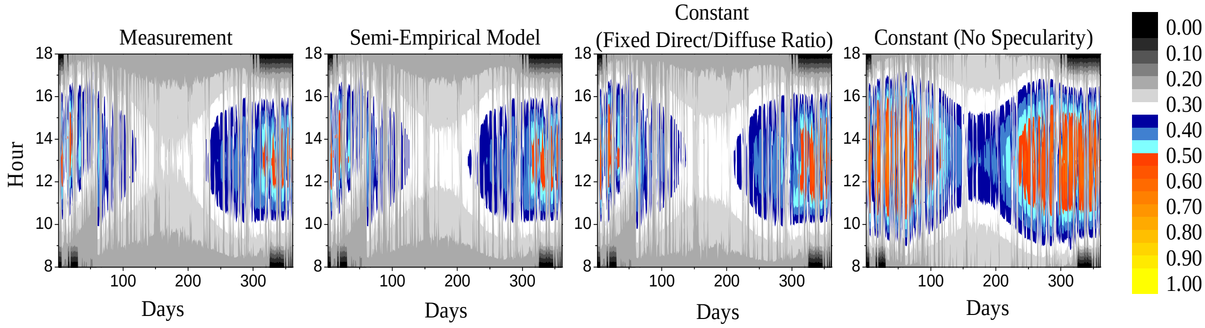

Figure 10: Annual DGP distribution with Fabric 4

Table 3 summarizes the results of annual daylighting simulation using different solar optical properties models. These results show that that the semi-empirical model can adequately capture the effect of angular properties and direct-diffuse fractions. On the contrary, both constant properties models will cause significant errors in daylight metrics and glare evaluation.

Table 3: Summary of Annual Daylighting Simulation results using Different Solar Optical Properties Models

	Fabric 3			Fabric 4		
	Continuous Daylight Autonomy	**Illuminance RMSE (lux)**	**Annual Time DGP > 0.35**	**Continuous Daylight Autonomy**	**Illuminance RMSE (lux)**	**Annual Time DGP > 0.35**
Detailed Measurements	0.32	#N/A	0.00	0.78	#N/A	0.21
Semi-Empirical Model	0.29	21.64	0.00	0.78	35.14	0.22
Constant (Fixed Beam/Diffuse Ratio)	0.48	193.19	0.00	0.89	641.19	0.27
Constant (No Specularity)	0.52	137.16	0.00	0.89	478.67	0.48

6. IMPACT OF PROPERTIES MODELING ON THE EFFECTIVENESS OF ADVANCED SHADING CONTROLS

An inaccurate model would affect the effectiveness of a control strategy, if the shading properties are embedded in the control algorithm. The "effective illuminance" control (Shen and Tzempelikos 2013) which is the latest study related to glare and illuminance control with roller shades is such an example. The method combines the concept of total "effective" illuminance transmitted through the shaded and unshaded parts of the window and moves the shades to intermediate positions in order to avoid excessive daylight on the work plane, as well to always protect occupants from direct sunlight (customized and depends on the occupant's seating position).

The semi-empirical model and the constant transmittance with fixed direction/diffuse ratio are compared here using this new type of control. The hybrid ray tracing and radiosity method calculates shade position and interior illuminance and DGP.

Figure 11 shows the differences of shading closing fractions (% of shaded window area) between the two approaches, using the semi-empirical model as a baseline. It was proved that constant transmittance with fixed direction/diffuse ratio tends to overestimate transmitted illuminance, so that method also tends to provide more conservative shade positions. The maximum difference is around 4%.

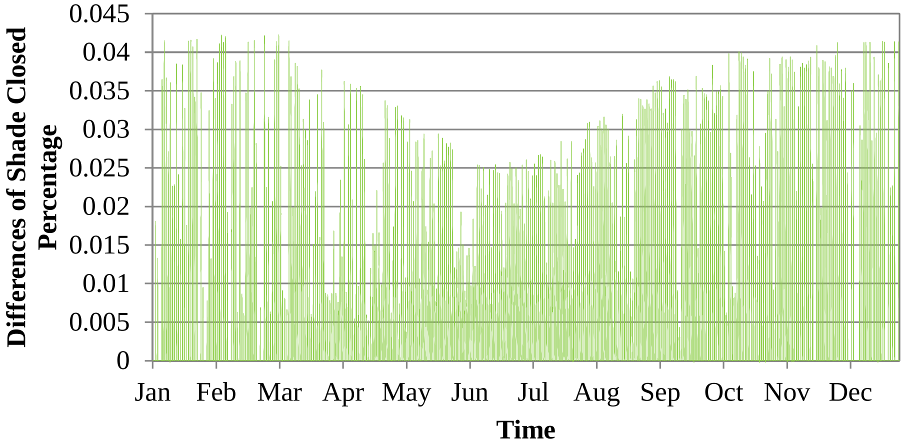

Figure 11: Differences of Shade Closed Percentage

Figure 12 presents the annual DGP distribution with controlled shades using the two models. The annual percentage of time when DGP exceeds 0.35 is 10% when the semi-empirical model is used and 7% when the constant model with fixed direct-diffuse ratio is used. There is also a 6% difference in continuous daylight autonomy between the two approaches. Therefore, incorrect modeling of solar optical properties affects the control methods and daylight metrics for controlled shades as well.

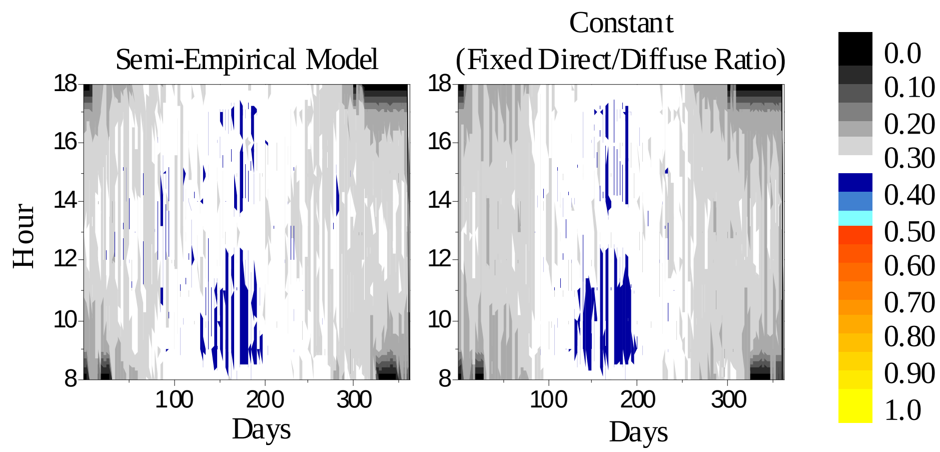

Figure 12: Annual DGP index when using different models to calculate shades positions

7. CONCLUSION

This paper first provides an overview of current approaches for modeling solar optical properties of roller shades, including advantages and limitations. Then, integrating sphere measurements were conducted to determine the detailed solar optical properties of different products. Measurement results for six roller shades fabrics are reported. The measurement results are compared to manufacturers' data and modeling results to better understand the accuracy of fabric datasheets and current modeling approaches. The comparison shows that the data provided by manufacturers is not always accurate and requires some careful review. The last part of the paper is a case study that demonstrates how the selection of modeling approaches could lead to issues in shading control.

Generally, the results confirm that the impacts of solar optical properties model on both daylighting and visual comfort are significant and should be considered as an important component in daylighting calculation modules. Kotey's semi-empirical model is performed well enough as a solar-optical properties predictor for roller shades. RMSE of illuminance prediction is small, and continuous daylight autonomy and annual high-DGP hour are both close to the results modelled using measured angular solar properties. Nevertheless, more investigations or modifications are necessary when it is applied to cases with reflective fabrics or solar incident angles between 65° and 90°.

On the contrary, using constant beam-total transmittance at normal incidence to model the solar optical properties causes significant errors on predictions of workplane illuminance and glare index in most cases. It would increase the chance of improper fenestration design and slightly influence the effectiveness of shading control. When applying constant properties models, correction factors are required, for example, using estimated diffuse-diffuse transmittance to replace beam-total transmittance at normal incidence.

The solar optical properties could also affect the calculation of peak cooling load and energy consumption. Detailed shading properties are recommended to be used for a more realistic evaluation of the impact of shading on energy use and visual comfort.

REFERENCES

Andersen, M. and de Boer, J. (2006). "Goniophotometry and Assessment of Bidirectional Photometric Properties of Complex Fenestration Systems." Energy and Buildings **38**(7): 836-848.

Andersen, M., Stokes, E., et al. (2010). "Using Digital Imaging to Assess Spectral Solar-Optical Properties of Complex Fenestration Materials: A New Approach in Video–Goniophotometry." Solar Energy **84**(4): 549-562.

Apian-Bennewitz, P. (2013). "Review of Simulating Four Classes of Window Materials for Daylighting with Non-Standard Bsdf Using the Simulation Program Radiance." Retrieved 04/08, 2014, from http://arxiv-web3.library.cornell.edu/abs/1307.4214.

Carli Inc. (2006). "Implementation of Wovenshade Method in Layeroptics.Dll." Retrieved 04/13, 2014, from http://windows.lbl.gov/software/window/Docs/Woven%20Shade%20Technical%20Documentation.pdf.

CGDB. (2014). "Complex Glazing Database " Retrieved 04/13, 2014, from http://windows.lbl.gov/software/CGDB/.

Chan, Y. C. and Tzempelikos, A. (2012). "A Hybrid Ray-Tracing and Radiosity Method for Calculating Radiation Transport and Illuminance Distribution in Spaces with Venetian Blinds." Solar Energy.

Collins, M., Wright, J., et al. (2012). "Off-Normal Solar Optical Property Measurements Using an Integrating Sphere." Measurement **45**(1): 79-93.

Deneyer, A., Deroisy, B., et al. (2014). "Bi-Directional Scattering Distribution Data of Solar Shading: Characterization and Performances." Retrieved 04/13, 2014, from http://www.cstc.be/homepage/download.cfm?dtype=research&doc=CIE_2013_Bi_Directional_Scattering_Distribution_of_solar_shading.pdf&lang=en.

EnergyPlus (2007). Energyplus Engineering Reference—the Reference for Energyplus Calculations, Lawrence Berkeley National Laboratory (LBNL).

IGDB. (2014). "International Glazing Database " Retrieved 04/13, 2014, from http://windows.lbl.gov/materials/IGDB/.

Jonsson, J. C., Lee, E. S., et al. (2008). Light-Scattering Properties of a Woven Shade-Screen Material Used for Daylighting and Solar Heat-Gain Control. Optical Engineering+ Applications, International Society for Optics and Photonics.

Kotey, N. A., Wright, J. L., et al. (2009). "A Detailed Model to Determine the Effective Solar Optical Properties of Draperies." ASHRAE Transactions **115**(1): 130-144.

Kotey, N. A., Wright, J. L., et al. (2009). "Determining Off-Normal Solar Optical Properties of Insect Screens." ASHRAE Transactions **115**(1): 155-164.

Kotey, N. A., Wright, J. L., et al. (2009). "Determining Off-Normal Solar Optical Properties of Roller Blinds." ASHRAE Transactions **115**(1): 145-154.

LBNL (2011) "Therm 6.3 / Window 6.3 Nfrc Simulation Manual."

McNeil, A., Jonsson, C. J., et al. (2013). "A Validation of a Ray-Tracing Tool Used to Generate Bi-Directional Scattering Distribution Functions for Complex Fenestration Systems." Solar Energy **98, Part C**(0): 404-414.

Nilsson, A. M. and Jonsson, J. C. (2010). "Light-Scattering Properties of a Venetian Blind Slat Used for Daylighting Applications." Solar Energy **84**(12): 2103-2111.

Reinhart, C. F. and Andersen, M. (2006). "Development and Validation of a Radiance Model for a Translucent Panel." Energy and Buildings **38**(7): 890-904.

Shen, H., Chan, Y. C., et al. (2013). Full-Scale Experimental Study of Lighting Performance with Automated Shading and Lighting Controls. ISES Solar World Congress 2013. Cancun, Mexico.

Shen, H. and Tzempelikos, A. (2012). "Daylighting and Energy Analysis of Private Offices with Automated Interior Roller Shades." Solar Energy **86**(2): 681-704.

Shen, H. and Tzempelikos, A. (2013). Evaluation of Shading Retrofit Strategies for Energy Savings in Office Buildings with Multiple Exterior Facades. CISBAT 2013. Lausanne, Switzerland.

Tzempelikos, A. and Shen, H. (2013). "Comparative Control Strategies for Roller Shades with Respect to Daylighting and Energy Performance." Building and Environment **67**: 179-192.

Wankanapon, P. and Mistrick, R. G. (2011). "Roller Shades and Automatic Lighting Control with Solar Radiation Control Strategies." BUILT **1**((1)).

Wienold, J. and Christoffersen, J. (2006). "Evaluation Methods and Development of a New Glare Prediction Model for Daylight Environments with the Use of Ccd Cameras." Energy and Buildings **38**(7): 743-757.

ACKNOWLEDGMENTS

The authors would like to thank Lutron Electronics Co Inc for supporting this work, and ASHRAE for providing resources through the new investigator award and a grant-in aid award. Many thanks to Prof. Michael Collins from the University of Waterloo for conducting the integrated sphere measurements for several roller shade materials.